NOTES AND CORRESPONDENCE

March 1987 Cyclone (Blizzard) over the Eastern Mediterranean and Balkan Region Associated with Blocking

METE TAYANÇ

Department of Environmental Engineering, Marmara University, Istanbul, Turkey

MEHMET KARACA AND H. NÜZHET DALFES

Istanbul Technical University, Eurasia Institute of Earth Sciences and Maden Fak. Genel Jeoloji ABD, Istanbul, Turkey

4 April 1997 and 11 October 1997

ABSTRACT

The March 1987 blizzard over the eastern Mediterranean and Balkan regions is investigated. Northern Hemispheric and regional 250- and 850-hPa geopotential heights illustrate the formation of blocking over northern Europe and cyclogenesis over the considered area. The 850-hPa analyses and National Centers for Environmental Prediction Eta model simulations are in good agreement. Temporal analyses of temperature and precipitation fields show that a cold air surge over the region resulted in a decrease in the daily temperatures of up to 15°C and a heavy accumulation of snow in the early days of the storm. Spatial analyses of the precipitation field reveal that the most snowfall-affected regions were northwestern Turkey and the Balkan countries.

1. Introduction

The persistent severe snow storm of March 1987 (also labeled ''the Storm of the Century'' by Turkish authorities) significantly disrupted human activity over a widespread area covering the Balkan regions and eastern Mediterranean. It was noted for its exceptional intensity over northwestern Turkey and the crucial role that the persistent high-latitude ridging event (commonly referred to as ''blocking'') played over northern Europe in the incipient cyclogenesis. The failure of the State Meteorological Office of Turkey to properly forecast the initial cyclogenesis, and the surge of cold air in the wake of the storm that reached North Africa and Middle East, compounded impacts of this event.

The relationship between atmospheric blocking and antecedent, upstream cyclone activity is a matter of considerable scientific interest (Dole 1989; Nakamura and Wallace 1990; Colucci and Alberta 1996) since this possible relationship was first suggested by Berggren et al. (1949). A blocking event may last for 15 days or more, but its onset and breakdown are usually considerably more rapid, on the order of 2–3 days (Dole 1989). The accurate prediction of the onset of blocking by numerical forecast models remains a formidable challenge (Tibaldi and Molteni 1990; Renwick and Wallace 1996).

The severe cyclones in the eastern Mediterranean that are associated with blocking over northern Europe are rare events but may cause blizzards if polar air penetrates into the region (Alpert and Reisin 1986). A prominent feature of these cyclones is their long persistence, generally more than a week. Many studies deal with cyclones and their trajectories over the Mediterranean (Wigley and Farmer 1982; Chang 1972) but only a few of them considered a significant case of cyclogenesis in the region (Buzzi and Tibaldi 1978; McGinley 1982; Alpert and Reisin 1986).

The purpose of this note is threefold:

1) to illustrate the evolution of the cyclogenesis associated with the baroclinic zone over the region using European Centre for Medium-Range Weather Forecasts (ECMWF) 250- and 850-hPa analyses and to determine if this is a case of explosive cyclogenesis (Sanders and Gyakum 1980),
2) to show that the Eta model of the National Centers for Environmental Prediction (NCEP) simulates this case with very high skill, and
3) to document its impacts on the environment.

We begin by considering the development of the deep cyclone that affected many countries of the eastern Mediterranean and the Balkan region, highlighting its major impacts. Then we compare the ECMWF analyses with Eta model simulations. After critically assessing the

Corresponding author address: Dr. Mete Tayanç, Department of Environmental Engineering, Marmara University, Kuyubaşi, Kadiköy, Istanbul 81040, Turkey.
E-mail: mtayanc@marun.edu.tr

simulations, we investigate the precipitation patterns and the temperature fluctuations in the region to show the intensity and the characteristics of this exceptional case of a blocked cyclone.

2. Data and methodology

The results presented here are largely based on records of 250- and 850-hPa height analyses from the ECMWF. Simulations are generated using the NCEP eta model. The NCEP Eta model was developed by Mesinger and Janjic during the last 15 years (Mesinger 1984; Mesinger et al. 1988; Janjic 1994). Recent studies showed that the model is quite successful in simulating mesoscale and synoptic-scale atmospheric phenomena (Lazic and Talenta 1988; Karaca and Dobricic 1997). The basic characteristic of this model is the use of the step-mountain eta coordinate (Mesinger et al. 1988). It is a generalization of the sigma coordinate, for a simple assignment of the surface values to unity at all grid points reduces the eta coordinate to the sigma coordinate. The coordinate is defined as

$$\eta = \frac{p - p_T}{p_S - p_T}\eta_S,$$

where

$$\eta_S = \frac{p_{\mathrm{rf}}(z_S) - p_T}{p_{\mathrm{rf}}(0) - p_T}.$$

Here p is the pressure; the subscripts T and S stand for the top and surface values of the model atmosphere, respectively; z is the geometric height; and $p_{rf}(z)$ is a suitably defined reference pressure as a function of z. The surface heights z_s are permitted to take only a discrete set of values, chosen so that mountains are constructed from the 3D grid boxes in the model. Extensive testing has shown that when the eta coordinate is used instead of the sigma coordinate, resulting forecasts are more accurate (Talenta et al. 1994).

Janjic (1990, 1994) implemented the physics package of the model. Basic characteristics of this package are as follows.

1) Mellor–Yamada level 2.5 closure approach is used to calculate the turbulent kinetic energy and the associated vertical fluxes (Mellor and Yamada 1974, 1982).
2) The modification of Betts–Miller adjustment scheme for cumulus convection is used for both deep and shallow convection (Betts and Miller 1986).
3) Parameterizations of both short- and longwave radiation are taken from those developed at the Goddard Laboratory for Atmospheres (Harshvardhan and Corsetti 1984).
4) Interactive clouds with random overlap are included.

NCEP eta model integration domain spans 20°N to 76°N latitude and 20°W to 80°E longitude with a horizontal grid size of 1°. In the vertical, the NCEP eta model has 32 levels, and the time step for this experiment is 2 min. The initial and boundary values are taken from initialized 0000 UTC analyses on 1 March 1987 from the Mass Archives Retrieval System (MARS) archives of the ECMWF. The model was integrated for 96 h starting from 0000 UTC 1 March. Forecasts are obtained by initializing the model at 0000 UTC 1 March and by taking the boundary values from the observations.

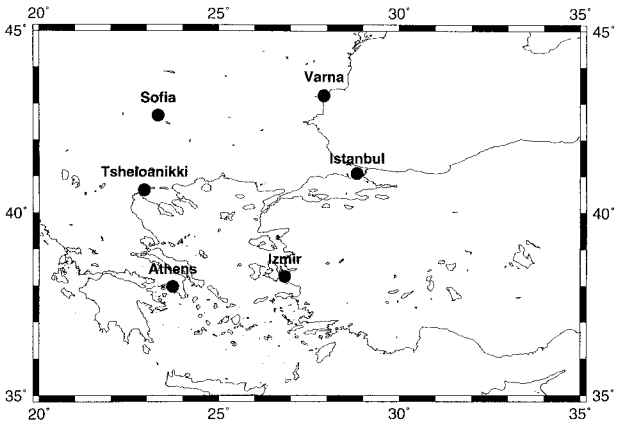

FIG. 1. The distribution of stations whose precipitation or temperature data is used in this study.

Station temperature and precipitation data together with the surface analyses for the considered period come from the State Meteorological Office of Turkey. The locations of stations whose data is used in this study is presented in Fig. 1. Detailed information about Turkish stations can be found in Karaca et al. (1995), Tayanç et al. (1997), and Tayanç and Toros (1997).

3. Results

a. Circulation patterns: The evolution of the cyclone and blocking

We focus on the 1–9 March period, during which the cyclogenesis started and the cyclone reached to its maximum activity. Figures 2a–d display a series of 250-hPa maps associated with wind vectors at 0000 UTC over the considered region for 1, 4, 6, and 8 March. A prominent geopotential low can be observed over northern Europe on 1 March and on the following days the trough of this system penetrated the eastern Mediterranean. The maximum wind trajectory at this level extends from United Kingdom to very low latitudes over Tunisia and Egypt, forming a high amplitude of the jetstream. On 4 March it can be observed that the center of the low having a value of 9417 moved toward the southwest. Two weak anticyclones start to form upstream and downstream of the cyclone on 6 March. The formation of a high pressure system over northern Europe and the Scandinavian countries steered this low toward the Med-

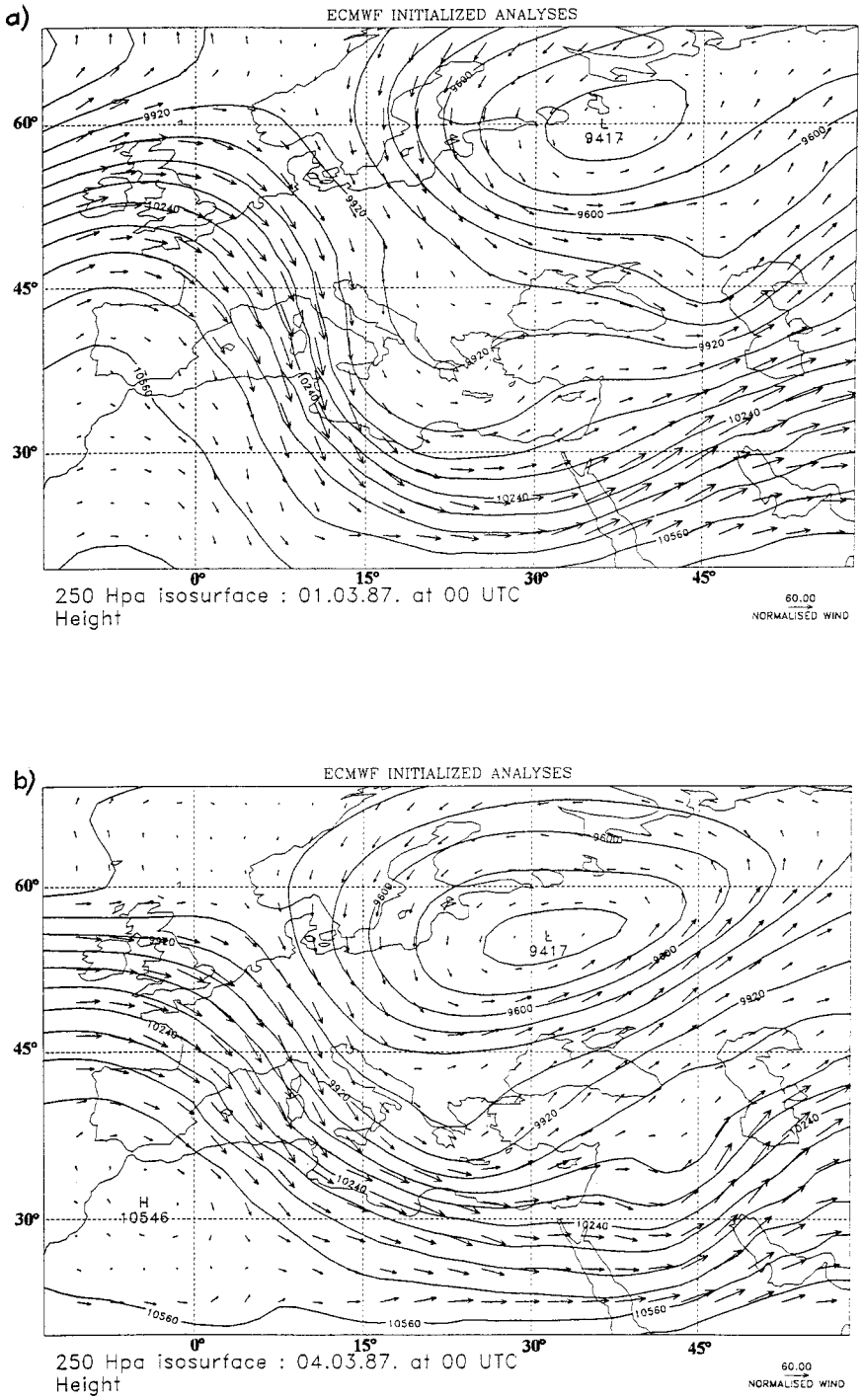

FIG. 2. ECMWF analyses of 250-hPa 0000 UTC geopotential height maps of Europe for (a) 1 March, (b) 4 March, (c) 6 March, and (d) 8 March 1987. Normalized wind values (kt) are depicted as arrows on the figures. Contour intervals are 10 m.

iterranean region. Owing to the intensification of the blocking, a deep, persistent, cold core cyclone formed over the eastern Mediterranean and Balkan region, where it stayed at least a week. A persistent anticyclone over northern Europe and its blocked cyclone located farther southward can be seen on 8 March. It is important to note the substantial amplification of the planetary-scale flow waves during the development phase of the cyclone that brought cold air to very low latitudes. The precipitation in the Balkan countries started on 3

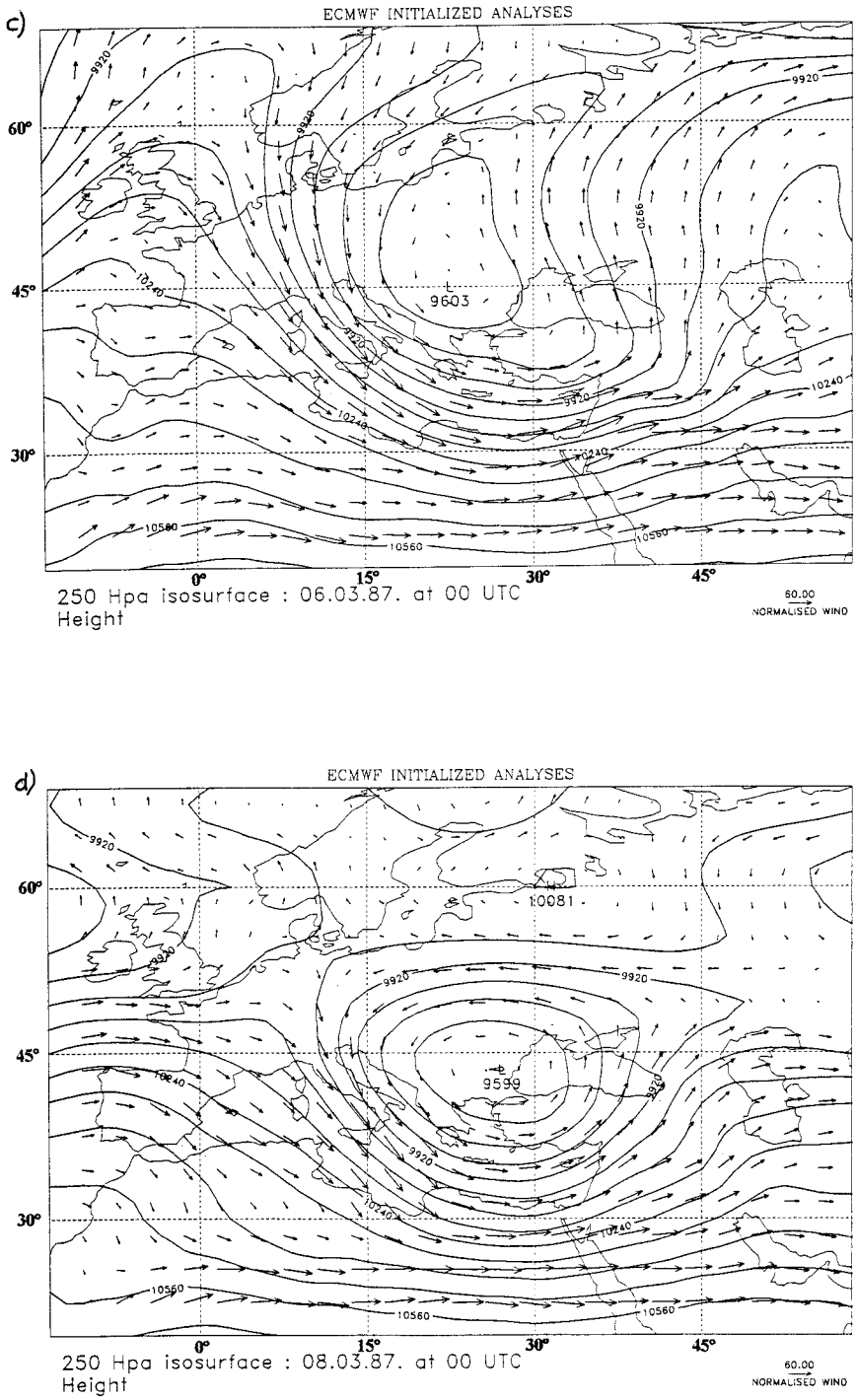

FIG. 2. (*Continued*)

March with snow storms moving to the southern areas on the following days. This cold weather intrusion is accompanied by unstable conditions that caused thunderstorms with snow showers in northwestern Turkey. Although the dissipation of the deep low pressure over the area started during the middle of March, the trough remained, and the precipitation over Turkey lasted well toward the end of the month while losing its intensity steadily.

Figure 3 displays the 850-hPa analysis, and 24- and 72-h forecasts at 0000 UTC from the NCEP eta model for the days of 1, 2 and 4 March, respectively. Similarly, Fig. 4 represents 850-hPa height patterns of the ECMWF analyses for the same dates. The solid lines

a)

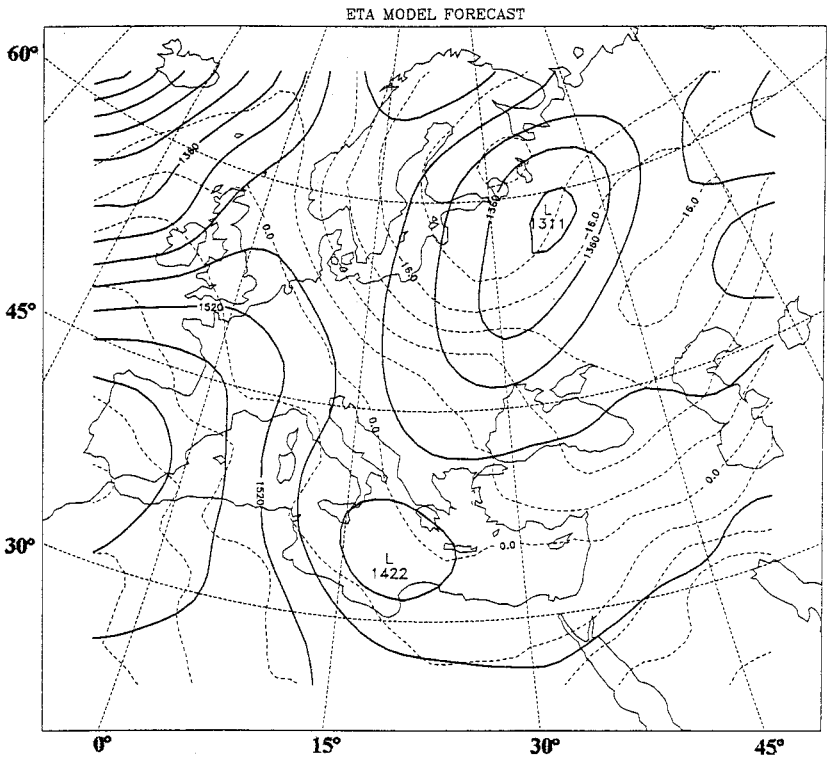

850 Hpa isosurface : 01.03.87. at 00 UTC + 00 h
Height (full line), temperature (dashed line)

b)

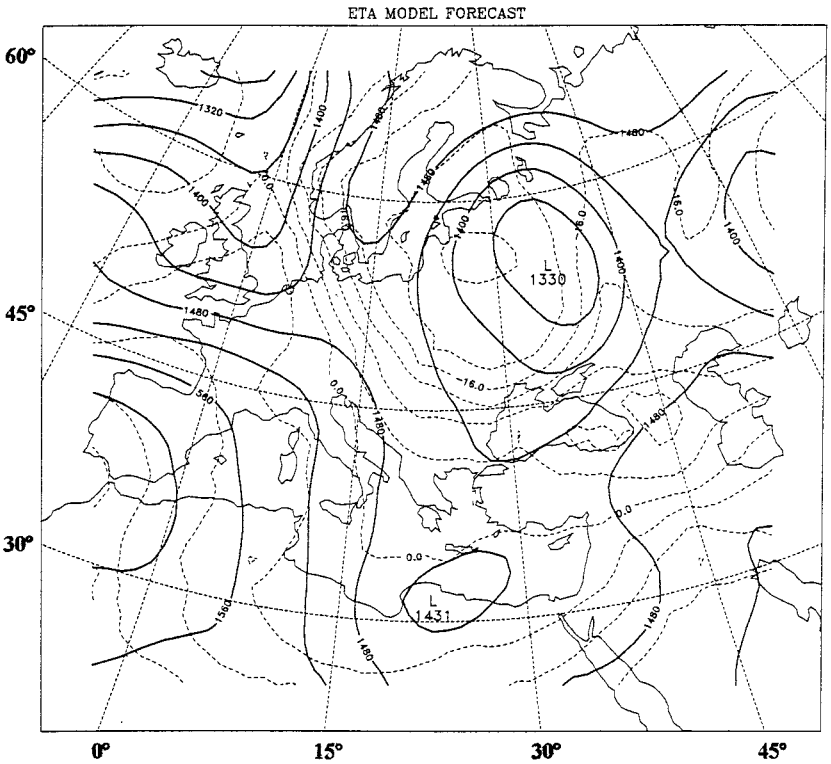

850 Hpa isosurface : 01.03.87. at 00 UTC + 24 h
Height (full line), temperature (dashed line)

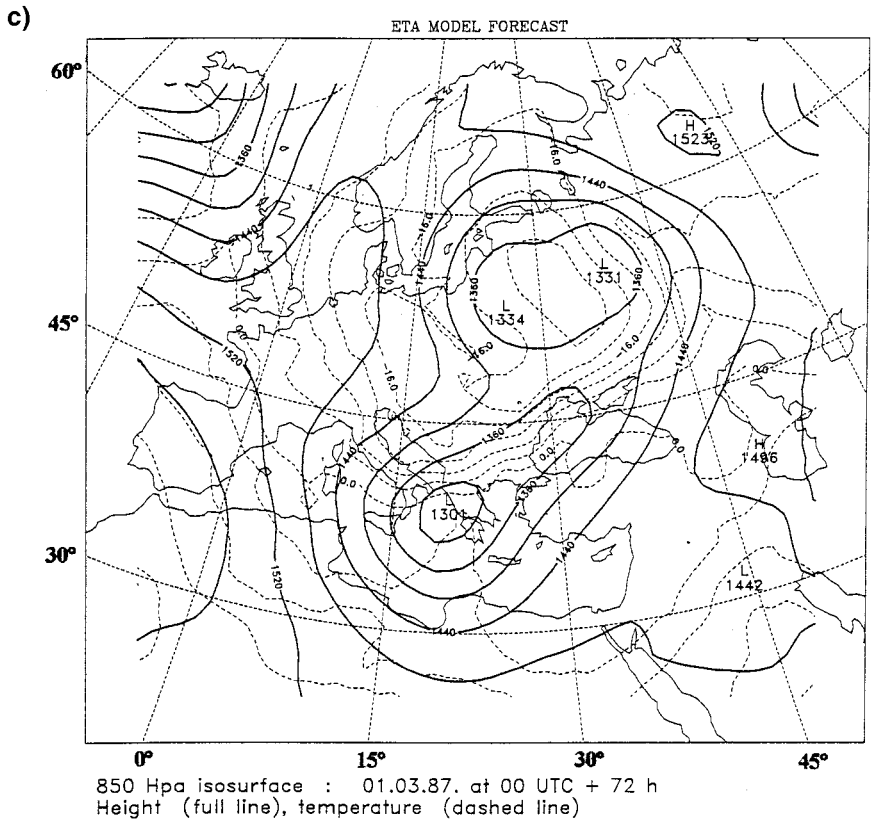

FIG. 3. (*Continued*)

in both figures represent the geopotential heights, and the dashed lines in Figs. 3 and 4 represent isotherms. The resulting geopotential height patterns generated by simulations and data analyses are very similar. The amplification of the large-scale flow and the baroclinic zone over the region containing warm and cold air very close to each other result in a quick cyclone formation with unstable conditions. Cold weather intrusion to the region produced a strong horizontal temperature gradient, which in turn caused the geostrophic wind speed to increase considerably with height. The maximum wind speed axis located at the highest geopotential gradient is highly correlated with these weather patterns.

Analogous to the 250-hPa height patterns, the 850-hPa height patterns on the days of 1 and 2 March illustrate a low pressure system over northern Europe and the trough associated with it that extends toward the Mediterranean. A weak cyclone can also be detected over northern Africa. ECMWF analysis and NCEP eta model forecasts show the motion of cold air to lower latitudes. The comparison of two days, 1 and 2 March, reveal that the isotherms having values below 0°C moved toward the Black Sea, intensifying the strength of the baroclinic condition. On 4 March, a strong cyclone is detected by ECMWF analysis and also by NCEP eta model forecasts at 850 hPa over the Aegean Sea, located west of Turkey, which is the culprit of the heavy snowfall. Analyses and forecasts for this day also illustrate the very large temperature gradient over the Balkan countries.

Figure 5 presents the surface analyses for the days of 1 and 4 March at 0000 UTC. On 1 March, a high pressure system is located over eastern Europe and a weak cyclone can be found over northern Africa. As expected from the upper air fields, low pressure starts to form over northwestern Turkey on the following day. Figure 5b depicts a very strong cyclone formed over southeastern Turkey on 4 March. Since this is a baroclinicly amplifying cyclone, the low pressure center at ground level is normally located farther east or southeast of the one located at higher altitudes, implying that the cyclone can further intensify. Very strong northerly and north-

←

FIG. 3. The 850-hPa geopotential heights and isotherms from the NCEP eta model forecasts for (a) 1 March, (b) 2 March, and (c) 4 March 1987. Geopotential heights are presented as solid lines with contour intervals of 40 m and isotherms as dashed lines with contour intervals of 3°C.

a)

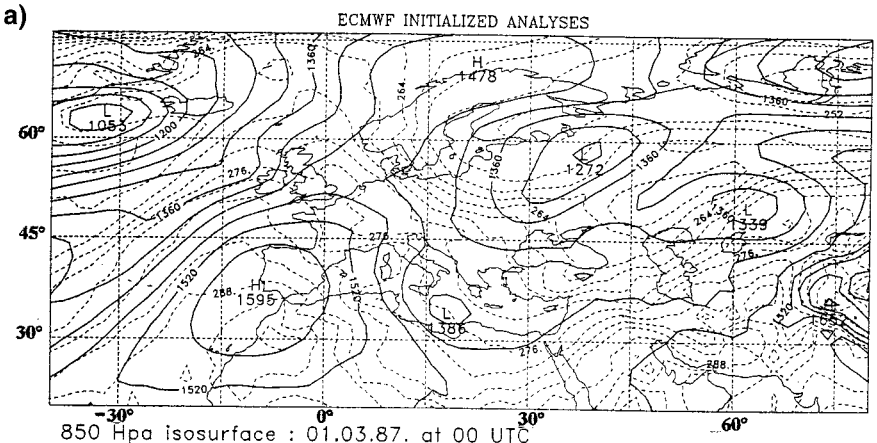

850 Hpa isosurface : 01.03.87. at 00 UTC
Height (full line), temperature (dashed line)

b)

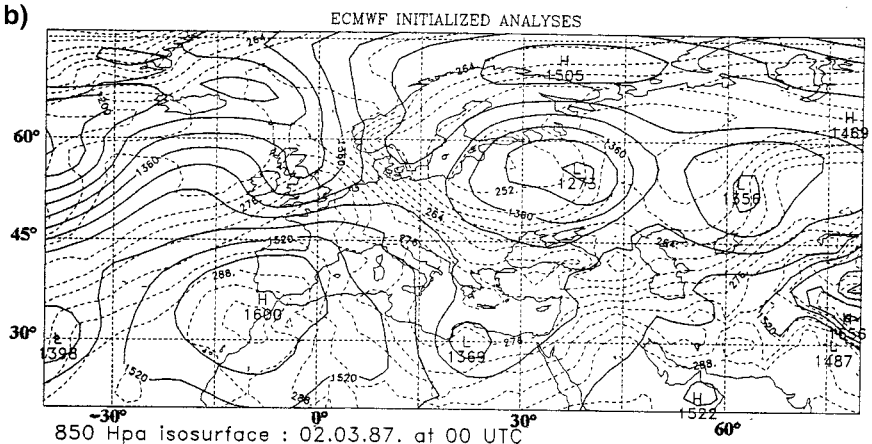

850 Hpa isosurface : 02.03.87. at 00 UTC
Height (full line), temperature (dashed line)

c)

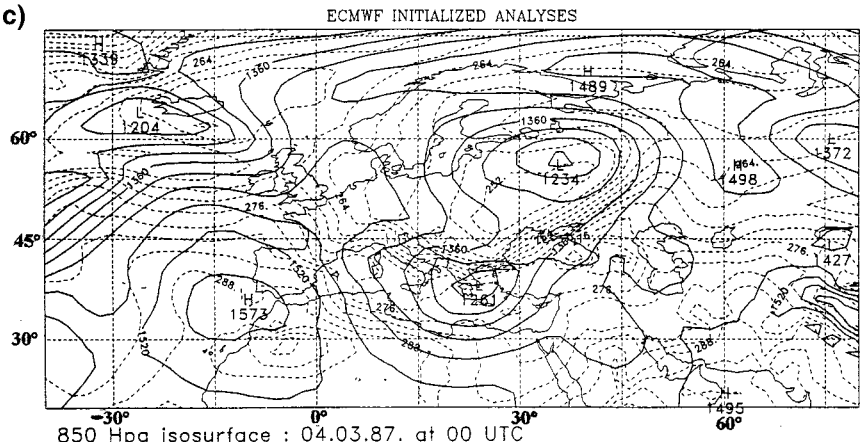

850 Hpa isosurface : 04.03.87. at 00 UTC
Height (full line), temperature (dashed line)

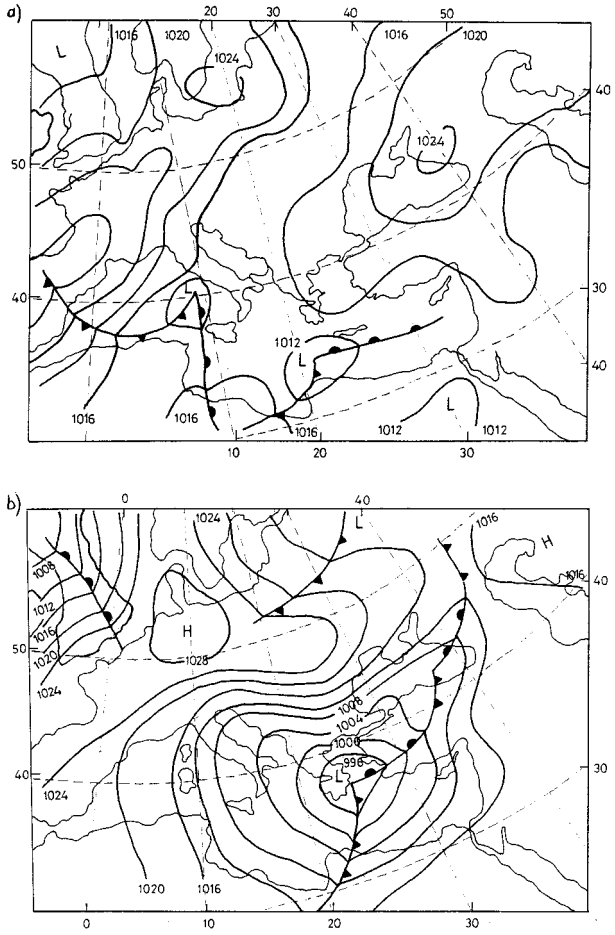

FIG. 5. Surface analyses for the days of (a) 1 March and (b) 4 March at 0000 UTC. Contour intervals are 4 hPa.

easterly winds observed in northwestern Turkey can easily be explained by the location of the low pressure system and by the pressure gradient found in the area. However, the surface pressure drop in the center of the cyclone on 4 March in a 24-h period (during the strongest phase of the deepening) multiplied by the ratio of the sine of the latitude divided by the sine of 60° does not exceed 20 mb. So it is intuitively clear that the March 1987 blizzard is not accociated with the explosive cyclogenesis phenomenon as described by Sanders and Gyakum (1980).

b. Consequences of the severe cyclone, precipitation amounts, temperature variability, and relationship with ENSO

The climax of the stormy weather over the area (in particular over Turkey) was on 4–6 March. İstanbul, the largest city of Turkey, got the biggest share of this event; the snow depth in many parts of the city reached 1 m on 7 March. The city was totally paralyzed by this blizzard; the intercity transportation and air traffic were brought to a standstill. Widespread heavy snowfall and very strong winds caused several deaths and a swath of material damage stretching from İstanbul to Zonguldak. Owing to the melting snow toward the end of March and the beginning of April, property losses were extensive, with hundreds of homes and workplaces flooded, roads were blocked, and many villages in the region were sequestered. Figure 6 shows the precipitation amounts at three stations in İstanbul. Precipitation is generally affected by topography and it is possible to have great variability of this parameter in a small area. The stations Kireçburnu, Kilyos, and Göztepe are located at least 20 km away from each other. Kilyos is located on the coast of the Black Sea, farther north of İstanbul in a rural area. Kireçburnu is on the coast of the Bosphorus in a suburban area, and Göztepe is located close to the shore of the Marmara Sea in the south, but a little bit inland in the urban center. Thus, it is possible to have this spatial variability of precipitation. It is clear that the majority of the precipitation fell during the 4–6 March period and was followed by a whole week of snowy weather with only short intermissions. This kind of extreme situation is a very rare event in İstanbul. Heavy snowfall and strong winds caused widespread damage to vegetation, breaking down branches of trees, and knocking down electricity poles.

The sudden temperature decrease observed on 3 March and the temperature change until 14 March in some cities of the Balkan region are presented in Fig. 7. A drop of 10°C or greater in daily mean temperatures clearly illustrates an abrupt polar air penetration to the region. The geopotential patterns in the previous figure show that very cold air from Siberia has moved over the region. On 7 and 10 March, very small amounts of precipitation are detected associated with warming in most stations, implying that either the cyclone may have lost its strength on these days or it may have moved farther north, resulting in the stations being positioned in the warm sector. But the other days illustrated in the figures have a considerable amount of precipitation and generally decreasing temperatures, implying that the cyclone may be in a deepening phase. Although the temperatures rose steadily until 14 March, the daily mean values remained below the freezing point in many cities, preventing the meltdown of the accumulated snow.

The spatial distribution of the simulated accumulated precipitation is shown in Figs. 8a–c. The heavy precipitation (greater than 25 mm) fell on western Turkey, the western Black Sea, and southeastern Greece. Middle

←

FIG. 4. The 850-hPa geopotential heights and isotherms from the ECMWF analyses for (a) 1 March, (b) 2 March, and (c) 4 March 1987. Geopotential heights are presented as solid lines with contour intervals of 40 m and isotherms as dashed lines with contour intervals of 3K.

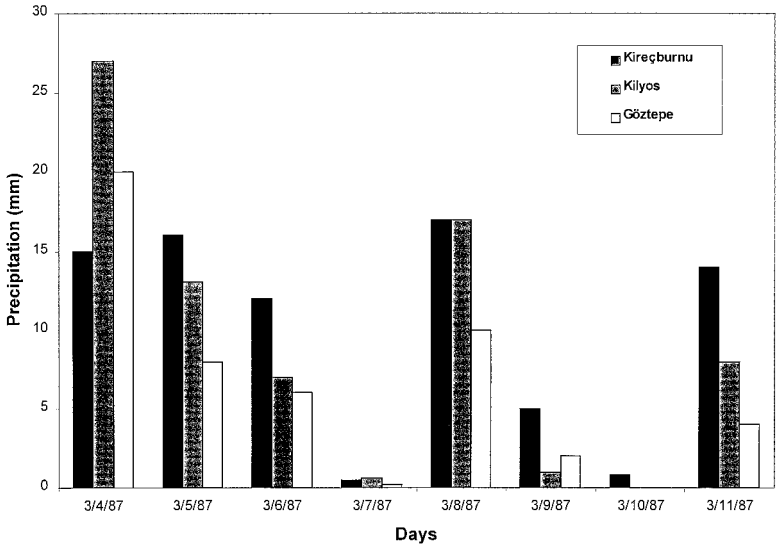

FIG. 6. Temporal variation of the precipitation amounts (mm) in the period of 4–11 March 1987 recorded in three meteorological stations located in İstanbul.

East countries also received precipitation owing to the trough of this deep cyclone. Generally, the snowy season in Turkey is the winter, and this is the first time that any İstanbul station had reported this amount of snow accumulation in the spring season. The month of March is usually characterized by precipitation deficiencies and seasonal warming in many parts of Turkey.

Van Loon and Madden (1981) and Renwick and Wallace (1996) found a relationship between blocking events and the phases of the ENSO cycle. The first study established a positive link between mean sea level pressures (SLPs) over the northern Atlantic and the warm phase of the ENSO cycle, implying that blocking may be enhanced over the North Atlantic during this phase. The latter found a negative relationship between the blocking cases over the North Pacific and the warm phase of the ENSO cycle. In this study, the extraordinary weather of March 1987 is found to correspond to

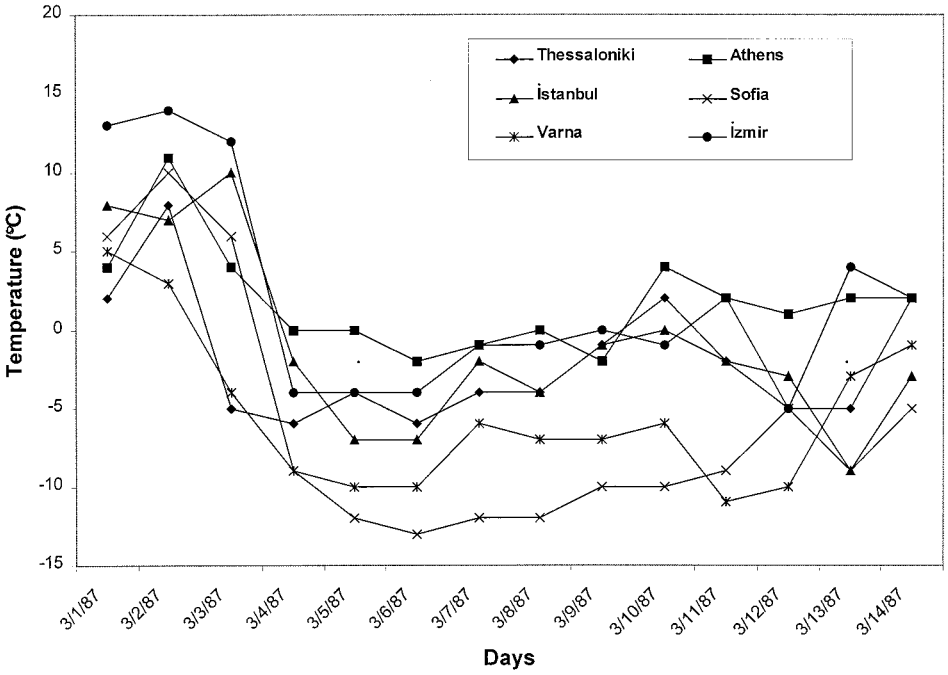

FIG. 7. Temporal variation of the daily mean temperatures (°C) in the period of 4–14 March 1987 recorded in the meteorological stations of the Balkan region.

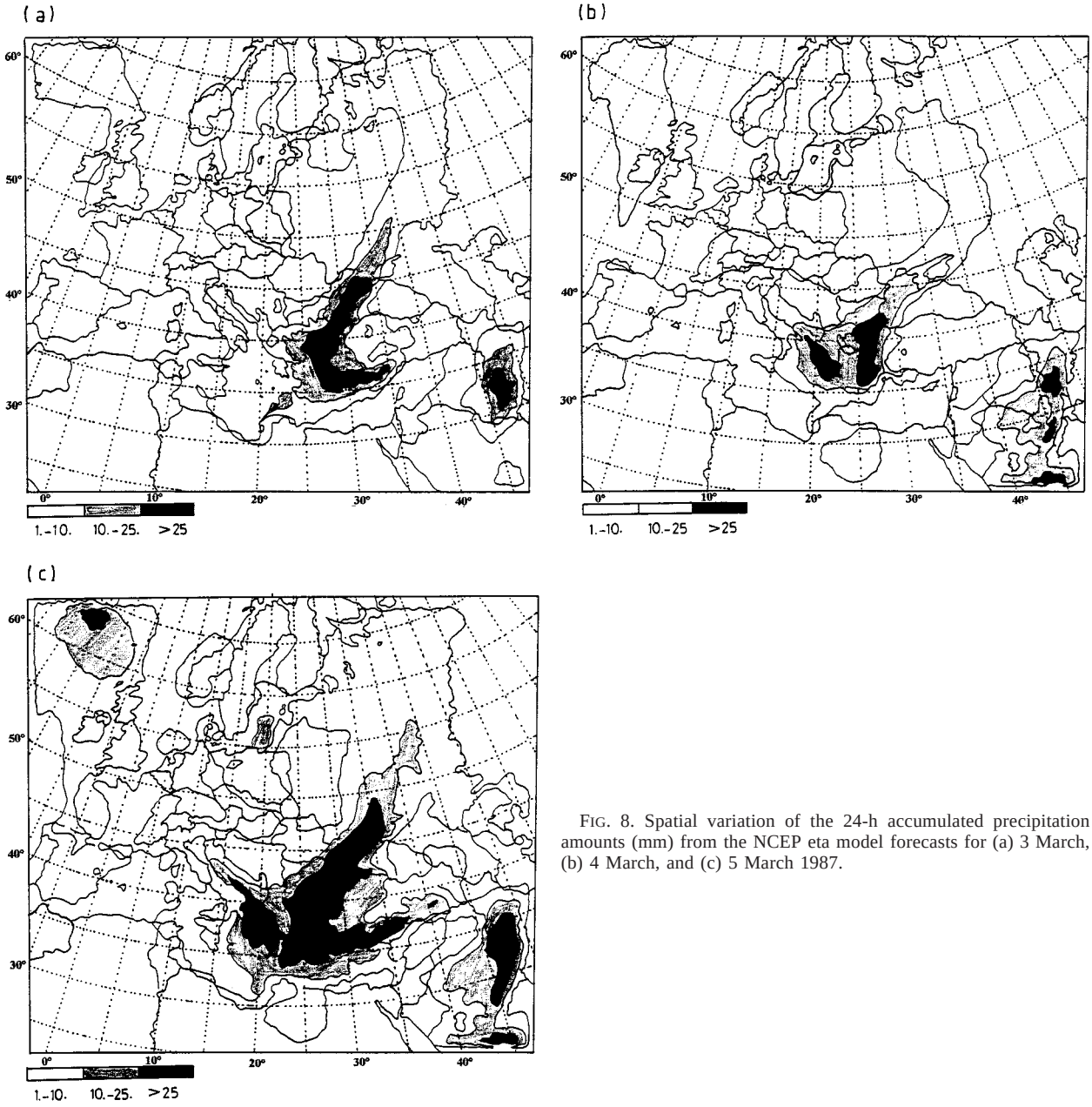

FIG. 8. Spatial variation of the 24-h accumulated precipitation amounts (mm) from the NCEP eta model forecasts for (a) 3 March, (b) 4 March, and (c) 5 March 1987.

a strong warm phase of the ENSO cycle. Figure 9 illustrates that the equatorial Pacific sea surface temperature (SST) anomalies are in the high positive range during the second half of 1986 and the first half of 1987 (WMO 1995). Similar to the February 1983 blizzard in the eastern Mediterranean, the March 1987 supercyclone also has a positive relationship with the warm phase of the ENSO cycle; though to prove this statement on statistical grounds, one will need much more data on blocking over northern Europe and deep cyclones in the eastern Mediterranean and will need to perform a thorough analysis.

4. Summary and conclusions

This study focused on the extreme weather event of the cyclogenesis over the eastern Mediterranean and the Balkan region. The trajectory of the polar air that penetrated into the area from the northeast is not a typical cold air transportation trajectory that affects the region (Alpert 1984).

The 250- and 850-hPa geopotential height analyses of ECMWF during 1–9 March 1987 revealed

1) the formation of extensive blocking over northern Europe,

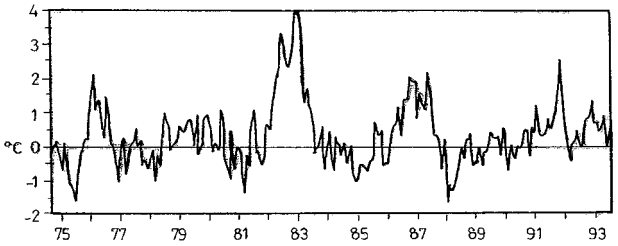

FIG. 9. Equatorial Pacific SST anomalies averaged over NINO 1 and 2 areas [adapted from WMO (1995)].

2) substantial amplification of the planetary-scale flow waves (Rossby waves),
3) very strong cyclogenesis over the eastern Mediterranean and Balkan region, and
4) a cold air surge to unusually low latitudes.

The 850-hPa geopotential height simulations of the NCEP eta model were found to be in good agreement with the analyses of ECMWF, even for the fourth day of the prediction period. This consistency suggests that the model performance for forecasting strong blocking and its accompanied rapid cyclogenesis in this region was highly acceptable at least in this case. The model results also depicted the formation of a baroclinic zone containing unstable air over the considered region.

Temporal analyses of surface air temperature at six stations in the considered region illustrate the abrupt decrease in temperature (up to 15°C) on the days of 3 and 4 March. Spatial analysis of precipitation showed that the areas with the greatest precipitation are northwestern Turkey and Balkan countries.

The cold outbreak to the region in March 1987 produced major adverse impacts on life; accumulated snow stopped the transportation leading to work hour losses, gale force winds blew off vegetation and damaged buildings, and the consumption of fuel for heating purposes reached its peak values. One beneficial impact of this weather was on water resources; increasing the water reserve of lakes, streams, and groundwater, providing additional supplies for drinking, irrigation, and electricity generation.

The blizzard of March 1987 and also a similar winter cyclone in 1983 were related to the strong warm phases of the ENSO cycle. Future predictions of the formation of severe cyclones with computer models and an assessment of their relationships with the certain global events require more in-depth studies.

Acknowledgments. We thank Ferruh Ertürk for giving us the inspiration for this work and Srdjan Dobricic for computational help in the earlier model runs. This study is a part of Projects YDABÇAG-519/A and 833, which are financially supported by Turkish Scientific and Technical Research Council (TÜBİTAK) and İ.T.U. Research Fund, respectively. It is also partially supported by TÜBİTAK's GloTek Research Unit.

REFERENCES

Alpert, P., 1984: An early winter subtropical cyclone in the eastern Mediterranean. *Israel J. Earth Sci.,* **33,** 150–156.
——, and T. Reisin, 1986: An early winter polar air mass penetration to the eastern Mediterranean. *Mon. Wea. Rev.,* **114,** 1411–1418.
Berggren, R., B. Bolin, and C. G. Rossby, 1949: An aerological study of zonal motion, its perturbation and breakdown. *Tellus,* **1,** 14–37.
Betts, A., and M. J. Miller, 1986: A new convective adjustment scheme. Part II: Single column tests using GATE wave, BOMEX, ATEX and Arctic air-mass data sets. *Quart. J. Roy. Meteor. Soc.,* **112,** 693–709.
Buzzi, A., and S. Tibaldi, 1978: Cyclogenesis in the lee of the Alps: A case study. *Quart. J. Roy. Meteor. Soc.,* **104,** 271–287.
Chang, J.-H., 1972: *Atmospheric Circulation Systems and Climate.* Oriental Publishing, 326 pp.
Colucci, S. J., and T. L. Alberta, 1996: Planetary-scale climatology of explosive cyclogenesis and blocking. *Mon. Wea. Rev.,* **124,** 2509–2520.
Dole, R. M., 1989: Life cycles of persistent anomalies. Part I: Evolution of 500-mb height fields. *Mon. Wea. Rev.,* **117,** 177–211.
Harshvardhan, and G. Corsetti, 1984: Longwave radiation parameterization for the UCLA/GLAS. NASA Tech. Memo. 86072, 48 pp.
Janjic, Z. I., 1990: The step-mountain coordinate: Physical package. *Mon. Wea. Rev.,* **118,** 1429–1443.
——, 1994: The step-mountain eta coordinate model: Further developments of the convection, viscous sublayer, and turbulence closure schemes. *Mon. Wea. Rev.,* **122,** 927–945.
Karaca, M., and S. Dobricic, 1997: Modeling of summertime meso-β scale cyclone in the Antalya Bay. *Geophys. Res. Lett.,* **24,** 151–155.
——, M. Tayanç, and H. Toros, 1995: The effects of urbanization on climate of İstanbul and Ankara. *Atmos. Environ.,* **29,** 3411–3421.
Lazic, L., and B. Talenta, 1990: Documentation of the UB/NMC Eta Model. WMO Tropical Meteorology Research Programme Tech. Doc. No. 366, WMO, Geneva, Switzerland, 307 pp.
McGinley, J., 1982: A diagnosis of Alpine lee cyclogenesis. *Mon. Wea. Rev.,* **110,** 1271–1287.
Mellor, G., and T. Yamada, 1974: A hierarchy of turbulence closure models for planetary boundary layers. *J. Atmos. Sci.,* **31,** 1791–1806.
——, and ——, 1982: Development of a turbulent closure models for geophysical fluid problems. *Rev. Geophys. Space Phys.,* **20,** 851–875.
Mesinger, F., 1984: A blocking technique for representation of mountains in atmospheric models. *Riv. Meteor. Aeronautica,* **44,** 195–202.
——, Z. Janjic, S. Nickovic, D. Gavrilov, and D. G. Deaven, 1988: The step mountain coordinate: Model description and performance for cases of Alpine lee cyclogenesis and performance for cases of an Appalachian redevelopment. *Mon. Wea. Rev.,* **116,** 1493–1518.
Nakamura, H., and J. M. Wallace, 1990: Observed changes in baroclinic wave activity during the life cycles of low-frequency circulation anomalies. *J. Atmos. Sci.,* **47,** 1100–1116.
Renwick, J. A., and J. M. Wallace, 1996: Relationships between North Pacific wintertime blocking, El Niño, and the PNA pattern. *Mon. Wea. Rev.,* **124,** 2071–2076.
Sanders, F., and J. R. Gyakum, 1980: Synoptic-dynamic climatology of the ''bomb.'' *Mon. Wea. Rev.,* **108,** 1589–1606.
Talenta, B., N. Aleksic, and M. Dacic, 1994: Application of the operational synoptic model for pollution forecasting in accidental situations. *Atmos. Environ.,* **28,** 2885–2891.
Tayanç, M., and H. Toros, 1997: Urbanization effects on regional climate change in the case of four large cities of Turkey. *Climate Change,* **35,** 501–524.
——, M. Karaca, and O. Yenigün, 1997: Annual and seasonal air

temperature trend patterns of climate change and urbanization effects in relation with air pollutants in Turkey. *J. Geophys. Res.*, **102,** 1909–1919.

Tibaldi, S., and F. Molteni, 1990: On the operational predictability of blocking. *Tellus*, **42A,** 343–365.

van Loon, H., and R. A. Madden, 1981: The Southern Oscillation. Part I: Global associations with pressure and temperature in northern winter. *Mon. Wea. Rev.*, **109,** 1150–1162.

Wigley, T. M. L., and G. Farmer, 1982: Climate of the eastern Mediterranean and the Near East. *Palaeoclimates, Palaeoenvironments and Human Communities in the Eastern Mediterranean Region in Later Prehistory*, J. L. Bintliff and W. Van Zeist, Eds., B. A. R. International Series, Vol. 133, British Archaeological Reports, 3–37.

WMO, 1995: *The Global Climate System Review*. World Climate Data and Monitoring Programme, 150 pp.